

Decuplet baryon magnetic moments in a QCD-based quark model beyond quenched approximation

Phuoc Ha*

*Physics Department, University of Wisconsin-Madison
Madison, Wisconsin 53706, USA*

Abstract

We study the decuplet baryon magnetic moments in a QCD-based quark model beyond quenched approximation. Our approach for unquenching the theory is based on the heavy baryon perturbation theory in which the axial couplings for baryon - meson and the meson-meson-photon couplings from the chiral perturbation theory are used together with the QM moment couplings. It also involves the introduction of a form factor characterizing the structure of baryons considered as composite particles. Using the parameters obtained from fitting the octet baryon magnetic moments, we predict the decuplet baryon magnetic moments. The Ω^- magnetic moment is found to be in good agreement with experiment: μ_{Ω^-} is predicted to be $-1.97\mu_N$ compared to the experimental result of $(-2.02 \pm 0.05) \mu_N$.

PACS Nos. 13.40.Em,11.30.Rd

Typeset using REVTeX

*Electronic address: phuoc@theory1.physics.wisc.edu

I. INTRODUCTION

The naive, nonrelativistic quark model (NQM), even though very simple in its formalism, is qualitatively good in describing the magnetic moments of the octet baryons. It fits the pattern and the general magnitude of the octet baryon moments up to $0.1\mu_N$ (nuclear magnetons) in average. The discrepancies between theoretical predictions and experimental data are due to the hadrons having an internal structure with a dynamically intricate properties that the NQM has not accounted for. Therefore, it is desirable to build a dynamical theory for the NQM.

In fact, the NQM can be derived from QCD using the Wilson loop approach [1]. By calculating the gauge invariant Green's function for a baryon interacting with an electromagnetic field and using well-defined approximations, such as the “quenched” approximation in which the internal virtual quark pair loops are not allowed and the minimal area law, we have derived the quark model for moments plus semi relativistic corrections associated with the binding of the quarks in the baryon. A test of this QCD-based QM by fitting the octet baryon moments showed that the theory failed to give any substantial improvement in the QM moments. The problem was identified with the quenched approximation [1].

To go beyond the quenched approximation, we have developed an loop expansion approach for the QCD-based QM and studied the octet baryon moments using our newly developed approach [2]. Our calculation is based on the heavy baryon perturbation theory in which the chiral baryon-meson couplings and the meson-meson-photon couplings from the chiral perturbation theory together with the QM moment couplings are used. It also involves the introduction of a single form factor characterizing the structure of the baryons considered as composite particles. The form factor reflects soft wave function effects with characteristic momenta at a scale $\lambda \sim 400$ MeV, well below the chiral cutoff ~ 1 GeV. We chose the strong interaction coupling constants in the chiral baryon-meson couplings to satisfy the SU(6) relations $F = 2/3D$, $C = -2D$, and $\mathcal{H} = -3D$, with $D = 0.75$ as would be expected for the $L = 0$ QM states. Our theory is convergent and has only three free parameters, the effective quark moments μ_u, μ_s , and the wave function parameter λ . The last is constrained by theory and experiment. In contrast the usual approaches to magnetic moments through ChPT [4,5,6,7] involve seven parameters in the description of the octet moments at one loop. If these parameters are used in fitting the seven measured octet moments, the effects of dynamical loop corrections appear only in the prediction for the $\Sigma^0\Lambda$ transition moment, where they are small [7].

We found in [2] that combining the dynamical corrections from the loop expansion with those associated with the binding of quarks in baryon significantly improved the agreement between the theoretical and experimental values of the baryon magnetic moments. The average deviation from fitting the seven well-measured octet magnetic moments excluding the transition moment $\mu_{\Lambda\Sigma^0}$, is $0.05\mu_N$, a substantial improvement on the QM. We concluded that the loop expansion is an effective way of going beyond quenched approximation in the octet baryon magnetic moment problem.

In this paper, we study the decuplet baryon magnetic moments using the same method. Our way of evaluating the semi relativistic corrections associated with the binding of quarks in the baryon and the choice of the strong interaction coupling constants and the octet - decuplet mass difference are the same for both octet and decuplet. We can therefore evaluate

the decuplet moments using the quark moments μ_u, μ_s , and the wave function parameter λ obtained in fitting the octet baryon moments, and predict the decuplet moments. In particular, the decuplet moment μ_{Ω^-} is predicted to be $-1.97\mu_N$ compared to the experimental result of $(-2.02 \pm 0.05)\mu_N$. The loop corrections are again small in comparison to the leading terms, and the contributions from the decuplet intermediate states are substantial in comparison to those from the octet intermediate states for some baryons.

The paper is organized as follows. Section II briefly describes loop expansion approach. An expression of the decuplet baryon magnetic moments are given in Sec. III, where some numerical results of calculating the decuplet baryon moments are also presented. The conclusions are given in Sec. IV. All the necessary formulae for the decuplet baryon moments can be found in the appendices.

II. LOOP EXPANSION APPROACH

Going beyond the quenched approximation in the QCD-based QM means that we have to develop an approach for studying the meson loop effects in the QCD-based QM. We also need to take the composite structure of the baryons into account. This is already included in the calculation of the QCD binding effects, but must also be included in the loop calculations. For that purpose, we introduce a single form factor characterizing the structure of the $L = 0$ baryons considered as composite particles. We base our loop calculations on heavy baryon perturbation theory (HBPT) and use, together with the QM moment couplings, chiral couplings for the low momentum couplings of mesons to baryons. That is, the couplings of the heavy baryon chiral perturbation theory (HBChPT) are used where chiral baryon-meson couplings and the meson-meson-electromagnetic field couplings are invoked, but the actual calculation of the loop graphs is modified with respect to [4], [5].

A. Definition of couplings

1. Chiral couplings

HBChPT, which has been used to study the hadronic processes of momentum transfers much less than 1 GeV, is well described in Refs. [8]. Let us consider a heavy baryon interacting with a low momentum meson. The velocity of the baryon is nearly unchanged when it exchanges some small momentum with the meson. Then, a nearly on-shell baryon with velocity v^μ has momentum

$$p^\mu = m_B v^\mu + k^\mu, \quad (2.1)$$

where m_B is the baryon mass, and $k \cdot v \ll m_B$. The effective heavy baryon theory is written in terms of baryon fields B_v with definite velocity v^μ , which are related to the original baryon fields by [8]

$$B_v(x) = e^{im_B v^\mu x_\mu} B(x). \quad (2.2)$$

The new baryon fields obey a modified Dirac equation,

$$i \not{\partial} B_v = 0 . \quad (2.3)$$

The chiral Lagrangian for baryon fields depends on the pseudoscalar meson octet

$$\phi = \frac{1}{\sqrt{2}} \begin{pmatrix} \frac{\pi^0}{\sqrt{2}} + \frac{\eta}{\sqrt{6}} & \pi^+ & K^+ \\ \pi^- & -\frac{\pi^0}{\sqrt{2}} + \frac{\eta}{\sqrt{6}} & K^0 \\ K^- & \bar{K}^0 & -\frac{2\eta}{\sqrt{6}} \end{pmatrix} , \quad (2.4)$$

which couples to the baryon fields through the vector and axial vector currents defined by

$$V_\mu = \frac{1}{f^2} (\phi \partial_\mu \phi - \partial_\mu \phi \phi) + \dots , \quad A_\mu = \frac{\partial_\mu \phi}{f} + \dots , \quad (2.5)$$

where $f \sim 93$ MeV is the meson decay constant. We will retain, as shown above, only leading term in the derivative expansion. The lowest order chiral Lagrangian for octet and decuplet baryons is then

$$\begin{aligned} \mathcal{L}_v = & i \text{Tr} \bar{B}_v (v \cdot \mathcal{D}) B_v + 2 D \text{Tr} \bar{B}_v S_v^\mu \{A_\mu, B_v\} + 2 F \text{Tr} \bar{B}_v S_v^\mu [A_\mu, B_v] \\ & - i \bar{T}_v^\mu (v \cdot \mathcal{D}) T_{v\mu} + \delta \bar{T}_v^\mu T_{v\mu} + \mathcal{C} \left(\bar{T}_v^\mu A_\mu B_v + \bar{B}_v A_\mu T_v^\mu \right) \\ & + 2 \mathcal{H} \bar{T}_v^\mu S_{v\nu} A^\nu T_{v\mu} + \text{Tr} \partial_\mu \phi \partial^\mu \phi + \dots , \end{aligned} \quad (2.6)$$

where δ is the decuplet-octet mass difference, and $\mathcal{D}_\mu = \partial_\mu + [V_\mu, \]$ is the covariant chiral derivative. B_v is the usual matrix of octet baryons, and the T_v^μ are the decuplet of baryons. D , F , \mathcal{C} , and \mathcal{H} are the strong interaction coupling constants. The spin operator S_v^μ is defined in Ref. [3]. This Lagrangian defines meson-baryon couplings we will use.

The meson-meson-electromagnetic field couplings and the convection current interactions of the baryons are introduced into the Lagrangian by making a substitutions:

$$\begin{aligned} \mathcal{D}_\mu & \rightarrow \mathcal{D}_\mu + ie \mathcal{A}_\mu [Q,] , \\ \partial_\mu \phi & \rightarrow \mathcal{D}_\mu \phi = \partial_\mu \phi + ie \mathcal{A}_\mu [Q, \phi] , \end{aligned} \quad (2.7)$$

where \mathcal{A}_μ is the photon field.

2. QM moment couplings

In order to employ the techniques of HBPT, we need octet, decuplet, and decuplet-octet transition magnetic moment operators which give the corresponding QM moments. We can construct these using B_v , T_v^μ , and the moment operator $\hat{Q} = \text{diag} (\mu_u, \mu_d, \mu_s)$ [2]. For example, the QM decuplet magnetic moment operator is

$$\mathcal{L}^{(3/2)} = -i \frac{3e}{2m_N} \bar{T}_{vijkl}^\mu \hat{Q}_j^i T_v^{\nu jkl} F^{\mu\nu} , \quad (2.8)$$

where i, j, k , and l are SU(3) flavor indices. In a momentum space, after doing a calculation on the flavor indices, we find that this operator reproduces the QM decuplet moments

$$\mathcal{L}_b^{(3/2)}(q) = \mu_b^{QM} I , \quad (2.9)$$

where q is the photon momentum and the spin dependent factor I is defined by

$$I = i\mu_N(\bar{T}' \cdot \mathcal{A}T' \cdot q - \bar{T}' \cdot qT' \cdot \mathcal{A}) . \quad (2.10)$$

The T' 's are defined and the factor is evaluated in Appendix A using the heavy baryon spin structure states. Note that the decuplet T' 's are now having the Dirac, spin and Lorentz indices only, $T' = T'_{\alpha,\lambda}^\mu$. The Dirac index α and spin index are suppressed. The QM decuplet moments μ_b^{QM} are

$$\begin{aligned} \mu_{\Delta^{++}}^{QM} &= 3\mu_u, & \mu_{\Delta^+}^{QM} &= 2\mu_u + \mu_d, & \mu_{\Delta^0}^{QM} &= 2\mu_d + \mu_u, & \mu_{\Delta^-}^{QM} &= 3\mu_d, \\ \mu_{\Sigma^{*+}}^{QM} &= 2\mu_u + \mu_s, & \mu_{\Sigma^{*0}}^{QM} &= \mu_u + \mu_d + \mu_s, & \mu_{\Sigma^{*-}}^{QM} &= 2\mu_d + \mu_s, \\ \mu_{\Xi^{*0}}^{QM} &= 2\mu_s + \mu_u, & \mu_{\Xi^{*-}}^{QM} &= 2\mu_s + \mu_d, \\ \mu_{\Omega^-}^{QM} &= 3\mu_s. \end{aligned} \quad (2.11)$$

The decuplet-octet transition magnetic moment operator is chosen as

$$\mathcal{L}^{(od)} = -i\frac{2e}{m_N}F^{\mu\nu}(\epsilon_{ijk}\hat{Q}_i^j\bar{B}_{vm}^jS_v^\mu T_v^{\nu klm} + h.c) , \quad (2.12)$$

which gives the decuplet-octet transition moments

$$\begin{aligned} \mu_{\Delta^+p} &= \frac{2\sqrt{2}}{3}(\mu_u - \mu_d) , & \mu_{\Delta^0n} &= \frac{2\sqrt{2}}{3}(\mu_u - \mu_d), \\ \mu_{\Sigma^{*+}\Sigma^+} &= \frac{2\sqrt{2}}{3}(\mu_s - \mu_u) , & \mu_{\Sigma^{*-}\Sigma^-} &= \frac{2\sqrt{2}}{3}(\mu_d - \mu_s) , \\ \mu_{\Sigma^{*0}\Sigma^0} &= \frac{\sqrt{2}}{3}(\mu_u + \mu_u - 2\mu_s) , & \mu_{\Sigma^{*0}\Lambda} &= \sqrt{\frac{2}{3}}(\mu_d - \mu_u) , \\ \mu_{\Xi^{*0}\Xi^0} &= \frac{2\sqrt{2}}{3}(\mu_s - \mu_u) , & \mu_{\Xi^{*-}\Xi^-} &= \frac{2\sqrt{2}}{3}(\mu_d - \mu_s) , \end{aligned} \quad (2.13)$$

that are the same as the QM results except for a change in sign of $\mu_{\Sigma^{*0}\Lambda}$ and $\mu_{\Xi^{*0}\Xi^0}$. This difference comes from a difference choice of the phases of the baryon fields, and does not affect to the calculations of the loop corrections for the baryon magnetic moments.

B. Meson Wave Function Effects - Form Factor

For investigating the meson wave function effects on the baryon moments, we introduce at each vertex with a meson line a form factor $F(k, v)$ defined in the rest frame of the heavy baryon by

$$F(k, v) = \frac{\lambda^2}{\lambda^2 + \mathbf{k}^2} , \quad (2.14)$$

where $k = (k_0, \mathbf{k})$ is the 4-momentum of meson and λ is a parameter characterizing a natural momentum scale for the wave function, expected to be much below 1 GeV. The form factor

defined as in Eq. (2.14) is normalized at chiral limit when \mathbf{k} is set equal to zero. With the introduction of this form factor, all the Feynman integrals give finite contributions. We therefore have a convergent theory in which the counterterms characteristic of loop calculations in ChPT are no longer necessary.

Our method for evaluating the Feynman integrals from the loop graphs (Figs. 1 and 2) with the form factors inserted is as follows.

First, we rewrite the form factor (2.14) in terms of k^μ and v^μ as

$$\frac{-\lambda^2}{k^2 - (k \cdot v)^2 - \lambda^2} . \quad (2.15)$$

Then, using the Feynman parametrization formula, we combine the factors in the denominator for the loop graph into a general form

$$k^2 + \alpha(k \cdot v)^2 + (k \cdot V) + C , \quad (2.16)$$

where α and C are parameters independent of the integral variables k , and the vector V is any combination of v and the photon momentum q . At this point, by changing variables to

$$k' = k + \beta v(k \cdot v) , \quad (2.17)$$

and choosing $\beta = \pm\sqrt{1+\alpha} - 1$, we can get rid of the $(k \cdot v)^2$ term in the denominator. Eq.(2.16) becomes

$$k'^2 + (k' \cdot \tilde{V}) + C . \quad (2.18)$$

where the vector \tilde{V} is also any combination of v and q . The Feynman integrals with the intergrands containing the denominators of this type are easily evaluated. Note that the Jacobian of the transformation of variables (Eq.(2.17)) is $1/\sqrt{1+\alpha}$.

III. DECUPLET BARYON MAGNETIC MOMENTS

A. Theoretical expressions

The calculation of the loop graphs shown in Figs. 1 and 2 is straightforward. The main difficulty is in the calculation of the ‘‘group coefficients’’ that arise from the products of couplings. These algebraic calculations were done using Mathematica and checked with some group coefficients given in [9]. The results are given in Appendix B. We will only give the final expressions for the decuplet baryon magnetic moments. In units of nuclear magnetons, an expression of baryon moments is given by

$$\mu_b = \mu_b^{(0)} + \mu_b^{(\delta=0)} + \mu_b^{(\delta \neq 0)} , \quad (3.1)$$

where $\mu_b^{(0)}$ are the contributions from the lowest loop order. These include the QM moments plus the corrections $\Delta\mu_b^{QM}$ from the QCD-based QM¹. The terms in $\mu_b^{(\delta=0)}$ are contributions

¹The explicit expressions of $\Delta\mu_b^{QM}$ are given in [1,2]

from the loop graphs which are independent of the decuplet-octet mass difference $\delta = m_B^{decuplet} - m_B^{octet}$ (here intermediate baryon states are purely decuplet), and the terms in $\mu_b^{(\delta \neq 0)}$ are contributions from the loop graphs dependent to δ (here intermediate baryon states are octet or octet and decuplet combined). We find

$$\begin{aligned} \mu_b^{(0)} &= \alpha_b + \Delta\mu_b^{QM} , \\ \mu_b^{(\delta=0)} &= \sum_{X=\pi,K} \frac{m_N}{72\pi f^2} \frac{\lambda^4}{(\lambda + m_X)^3} \beta_b^{(X)} \\ &+ \sum_{X=\pi,K,\eta} \frac{1}{16\pi^2 f^2} (\gamma_b^{1(X)} - 2\lambda_b^{(X)} \alpha_b) L_0(m_X, \lambda) , \end{aligned} \quad (3.2)$$

$$(3.3)$$

and

$$\begin{aligned} \mu_b^{(\delta \neq 0)} &= \sum_{X=\pi,K} -\frac{m_N}{16\pi f^2} \tilde{F}(m_X, -\delta, \lambda) \tilde{\beta}_b^{(X)} \\ &+ \sum_{X=\pi,K,\eta} \frac{1}{32\pi^2 f^2} \left[(\tilde{\gamma}_b^{1(X)} - 2\tilde{\lambda}_b^{(X)} \alpha_b) L_1(m_X, -\delta, \lambda) + \tilde{\gamma}_b^{2(X)} L_2(m_X, -\delta, \lambda) \right] , \end{aligned} \quad (3.4)$$

where $\alpha_b = \mu_b^{QM}$, and the group coefficients $\beta_b^{(X)}$, $\tilde{\beta}_b^{(X)}$, $\lambda_b^{(X)}$, $\tilde{\lambda}_b^{(X)}$, $\gamma_b^{1(X)}$, $\tilde{\gamma}_b^{1(X)}$, and $\tilde{\gamma}_b^{2(X)}$ are given in the appendix B.

Analytic expressions for $L_0(m_X, \lambda)$, $\tilde{F}(m_X, \delta, \lambda)$, $L_1(m_X, \delta, \lambda)$, and $L_2(m_X, \delta, \lambda)$, which are the functions of the meson masses, the decuplet-octet mass difference δ , and the natural cutoff λ , are given in [2]. It is straightforward to get $\tilde{F}(m_X, -\delta, \lambda)$, $L_1(m_X, -\delta, \lambda)$, and $L_2(m_X, -\delta, \lambda)$ from these expressions given, and such an example is shown in Appendix C. To have an idea which corrections come from which loop graphs (Figs. 1 and 2), it is necessary to know that $\beta_b^{(X)}$, $\tilde{\beta}_b^{(X)}$, $\gamma_b^{1(X)}$, $\tilde{\gamma}_b^{1(X)}$, $\tilde{\gamma}_b^{2(X)}$, $\lambda_b^{(X)}$, and $\tilde{\lambda}_b^{(X)}$ are the group coefficients of the graphs 1a, 1b, 2a, 2b, 2c (or 2d), 2e and 2f, respectively.

B. Numerical results

Now we are ready to evaluate the decuplet baryon magnetic moments. As done in the octet moment case, the corrections $\Delta\mu_b^{QM}$ from the QCD-based QM are calculated using the values of ϵ 's and Δ 's given in [7]. Again, for the loop corrections, the coupling constants F , D , \mathcal{C} , and \mathcal{H} were chosen such that $F + D = 1.25 \approx |g_A/g_V|$ (g_A and g_V are the axial vector and vector coupling constants, respectively) and the $SU(6)$ relations between the coupling constants $F = 2D/3$, $\mathcal{C} = -2D$, and $\mathcal{H} = -3D$ are satisfied, as expected for $L = 0$ baryons. We also choose the decuplet-octet mass difference $\delta = 250$ MeV and $f_\pi = 93$ MeV, $f_K = f_\eta = 1.2f_\pi$. The remaining three parameters μ_u , μ_s , and the natural cutoff λ are given the values that give the best fit in the octet moment case, namely $\mu_u = 2.803\mu_N$, $\mu_s = -0.656\mu_N$, and $\lambda = 407$ MeV.

We give our calculated values for the decuplet baryon magnetic moments, and the corresponding values from the NQM, in Table I and a detailed breakdown of the contributions of the loop integrals to the magnetic moments in Table II. We find that the *predicted* decuplet moment $\mu_{\Omega^-} = -1.97\mu_N$ is in very good agreement with the experimental result of $(-2.02$

± 0.05) μ_N , and the theoretical value of $\mu_{\Delta^{++}} = 5.69\mu_N$ falls within the experimental range (from 3.7 to 7.5 in unit of nuclear magnetons)

As in the octet case, again we see that the loop contributions are small in comparison to the tree level or QM terms, that the contributions from the graphs involving the intermediate decuplet states (sum of the graphs 1a, 2a, 2c, 2d, and 2e) are substantial. For some baryons, those contributions are even larger than those from the graphs involving only the intermediate octet states.

IV. CONCLUSIONS

In this paper, we have extended our earlier calculations of the octet baryon moments in a QCD-based QM with loop corrections to include the decuplet baryon magnetic moments. We have predicted the decuplet moments using the input parameters obtained from studying the octet baryon moments. We find that our predicted decuplet moment μ_{Ω^-} is in very good agreement with its experimental value.

Again, we have shown that our loop approach for baryon magnetic moments in a QCD-based QM works. The loop corrections extend our QCD-based QM beyond the quenched approximation. The resulting theory describes the baryon magnetic moments much better than the NQM. It can fit the seven observed octet baryon magnetic moments up to about $0.05\mu_N$ in average magnitude, gives a result for the $\Sigma^0\Lambda$ transition moment consistent with experiment, and predicts μ_{Ω^-} very well. We hope that the other decuplet baryon moments predicted from our theory will be tested by the future experimental data.

ACKNOWLEDGMENTS

The author would like to thank Professor Loyal Durand for helpful discussions and valuable supports. This work was supported in part by the U.S. Department of Energy under Grant No. DE-FG02-95ER40896.

APPENDIX A: HEAVY BARYON SPIN STRUCTURE

In a rest frame of a spin- $\frac{3}{2}$ baryon, the states $|j, j_z\rangle$ of this baryon are specified by a vector \mathbf{e} and a spin- $\frac{1}{2}$ spinor ξ_m , $m = -\frac{1}{2}, \frac{1}{2}$ as follows

$$\begin{aligned}
|\frac{3}{2}, \frac{3}{2}\rangle &= \mathbf{e}_{+1}\xi_{\frac{1}{2}}, \\
|\frac{3}{2}, \frac{1}{2}\rangle &= \frac{1}{\sqrt{3}}\mathbf{e}_{+1}\xi_{-\frac{1}{2}} + \sqrt{\frac{2}{3}}\mathbf{e}_0\xi_{\frac{1}{2}}, \\
|\frac{3}{2}, -\frac{1}{2}\rangle &= \sqrt{\frac{2}{3}}\mathbf{e}_0\xi_{-\frac{1}{2}} + \frac{1}{\sqrt{3}}\mathbf{e}_{-1}\xi_{\frac{1}{2}}, \\
|\frac{3}{2}, -\frac{3}{2}\rangle &= \mathbf{e}_{-1}\xi_{-\frac{1}{2}}.
\end{aligned} \tag{A1}$$

These states are satisfied the expected orthogonality and normalization properties. In terms of the vector-spinor functions $T' = T'_{\alpha, \lambda}$ with α a Dirac spinor index and $\lambda = j_z$ a total spin index, the state $|\frac{3}{2}, \frac{3}{2}\rangle$ is identified as

$$|\frac{3}{2}, \frac{3}{2}\rangle = T'_{\frac{1}{2}, \frac{3}{2}} = -\frac{1}{\sqrt{2}}(T'_{\frac{1}{2}, \frac{3}{2}}^x + iT'_{\frac{1}{2}, \frac{3}{2}}^y), \tag{A2}$$

and so on.

Consider the factor $I = i\mu_N(\bar{T}' \cdot \mathcal{A}T' \cdot q - \bar{T}' \cdot qT' \cdot \mathcal{A})$ that appears in Eq. (2.10). In the baryon rest frame $T'^{\mu} = (0, \mathbf{T}')$, while $\mathcal{A} = (0, \mathbf{A})$ for a pure magnetic field, then the factor I reduces to form

$$\begin{aligned}
I &= i\mu_N(\mathbf{T}'^* \cdot \mathbf{A}\mathbf{T}' \cdot \mathbf{q} - \mathbf{T}'^* \cdot \mathbf{q}\mathbf{T}' \cdot \mathbf{A}), \\
&= i\mu_N(\mathbf{T}'^* \times \mathbf{T}') \cdot (\mathbf{A} \times \mathbf{q}), \\
&= \mu_N(\mathbf{T}'^* \times \mathbf{T}') \cdot \mathbf{B},
\end{aligned} \tag{A3}$$

where $\mathbf{B} = i(\mathbf{A} \times \mathbf{q})$ is the magnetic field. By choosing the magnetic field along the \mathbf{e}_0 direction, $\mathbf{B} = \mathbf{e}_0 B$, then it follows from (A1) and (A3)

$$\begin{aligned}
I &= \pm i\mu_N B \quad \text{for } j_z = \pm \frac{3}{2}, \\
&= \pm i\mu_N \frac{B}{3} \quad \text{for } j_z = \pm \frac{1}{2}.
\end{aligned} \tag{A4}$$

Using (A1), we can check the validity of the following relation which is useful when evaluating some loop graphs

$$\bar{T}'^{\mu} [q \cdot S_v, \mathcal{A} \cdot S_v] T'_{\mu} = \frac{1}{2}(\bar{T}' \cdot \mathcal{A}T' \cdot q - \bar{T}' \cdot qT' \cdot \mathcal{A}), \tag{A5}$$

where S_v is the spin operator.

APPENDIX B: THE GROUP COEFFICIENTS

In this appendix, the group coefficients are presented explicitly. For simplicity, the superscript (X) is suppressed. The group coefficients β_b evaluated from the graphs 1a, up to a factor \mathcal{H}^2 , are

$$\begin{aligned}
 \beta_{\Delta^{++}}^{(\pi)} &= \frac{1}{3}, & \beta_{\Delta^+}^{(\pi)} &= \frac{1}{9}, & \beta_{\Delta^0}^{(\pi)} &= -\frac{1}{9}, & \beta_{\Delta^-}^{(\pi)} &= -\frac{1}{3}, \\
 \beta_{\Sigma^{*+}}^{(\pi)} &= \frac{2}{9}, & \beta_{\Sigma^{*0}}^{(\pi)} &= 0, & \beta_{\Sigma^{*-}}^{(\pi)} &= -\frac{2}{9}, \\
 \beta_{\Xi^{*0}}^{(\pi)} &= \frac{1}{9}, & \beta_{\Xi^{*-}}^{(\pi)} &= -\frac{1}{9}, \\
 \beta_{\Omega^-}^{(\pi)} &= 0,
 \end{aligned} \tag{B1}$$

for the pion loops,

$$\begin{aligned}
 \beta_{\Delta^{++}}^{(K)} &= \frac{1}{3}, & \beta_{\Delta^+}^{(K)} &= \frac{2}{9}, & \beta_{\Delta^0}^{(K)} &= \frac{1}{9}, & \beta_{\Delta^-}^{(K)} &= 0, \\
 \beta_{\Sigma^{*+}}^{(K)} &= \frac{1}{9}, & \beta_{\Sigma^{*0}}^{(K)} &= 0, & \beta_{\Sigma^{*-}}^{(K)} &= -\frac{1}{9}, \\
 \beta_{\Xi^{*0}}^{(K)} &= -\frac{1}{9}, & \beta_{\Xi^{*-}}^{(K)} &= -\frac{2}{9}, \\
 \beta_{\Omega^-}^{(K)} &= -\frac{1}{3},
 \end{aligned} \tag{B2}$$

for the kaon loops. The group coefficients $\tilde{\beta}_b$ evaluated from the graphs 1b, up to a factor \mathcal{C}^2 , are

$$\begin{aligned}
 \tilde{\beta}_{\Delta^{++}}^{(\pi)} &= 1, & \tilde{\beta}_{\Delta^+}^{(\pi)} &= \frac{1}{3}, & \tilde{\beta}_{\Delta^0}^{(\pi)} &= -\frac{1}{3}, & \tilde{\beta}_{\Delta^-}^{(\pi)} &= -1, \\
 \tilde{\beta}_{\Sigma^{*+}}^{(\pi)} &= \frac{2}{3}, & \tilde{\beta}_{\Sigma^{*0}}^{(\pi)} &= 0, & \tilde{\beta}_{\Sigma^{*-}}^{(\pi)} &= -\frac{2}{3}, \\
 \tilde{\beta}_{\Xi^{*0}}^{(\pi)} &= \frac{1}{3}, & \tilde{\beta}_{\Xi^{*-}}^{(\pi)} &= -\frac{1}{3}, \\
 \tilde{\beta}_{\Omega^-}^{(\pi)} &= 0,
 \end{aligned} \tag{B3}$$

for the pion loops,

$$\begin{aligned}
 \tilde{\beta}_{\Delta^{++}}^{(K)} &= 1, & \tilde{\beta}_{\Delta^+}^{(K)} &= \frac{2}{3}, & \tilde{\beta}_{\Delta^0}^{(K)} &= \frac{1}{3}, & \tilde{\beta}_{\Delta^-}^{(K)} &= 0, \\
 \tilde{\beta}_{\Sigma^{*+}}^{(K)} &= \frac{1}{3}, & \tilde{\beta}_{\Sigma^{*0}}^{(K)} &= 0, & \tilde{\beta}_{\Sigma^{*-}}^{(K)} &= -\frac{1}{3}, \\
 \tilde{\beta}_{\Xi^{*0}}^{(K)} &= -\frac{1}{3}, & \tilde{\beta}_{\Xi^{*-}}^{(K)} &= -\frac{2}{3}, \\
 \tilde{\beta}_{\Omega^-}^{(K)} &= -1,
 \end{aligned} \tag{B4}$$

for the kaon loops. The group coefficients γ_b^1 evaluated from the graphs 2a, up to a factor $11\mathcal{H}^2/9$, are

$$\begin{aligned}
\gamma_{\Delta^{++}}^{1(\pi)} &= 2\mu_u, & \gamma_{\Delta^+}^{1(\pi)} &= \frac{13}{12}\mu_u, & \gamma_{\Delta^0}^{1(\pi)} &= \frac{\mu_u}{6}, & \gamma_{\Delta^-}^{1(\pi)} &= -\frac{3}{4}\mu_u, \\
\gamma_{\Sigma^{*+}}^{1(\pi)} &= \frac{1}{9}(5\mu_u + 4\mu_s), & \gamma_{\Sigma^{*0}}^{1(\pi)} &= \frac{2}{9}(\mu_u + 2\mu_s), & \gamma_{\Sigma^{*-}}^{1(\pi)} &= \frac{1}{9}(-\mu_u + 4\mu_s), \\
\gamma_{\Xi^{*0}}^{1(\pi)} &= \frac{\mu_s}{3}, & \gamma_{\Xi^{*-}}^{1(\pi)} &= \frac{1}{12}(\mu_u + 4\mu_s), \\
\gamma_{\Omega^-}^{1(\pi)} &= 0,
\end{aligned} \tag{B5}$$

for the pion loops,

$$\begin{aligned}
\gamma_{\Delta^{++}}^{1(K)} &= \frac{1}{3}(2\mu_u + \mu_s), & \gamma_{\Delta^+}^{1(K)} &= \frac{1}{3}(\mu_u + \mu_s), & \gamma_{\Delta^0}^{1(K)} &= \frac{\mu_s}{3}, & \gamma_{\Delta^-}^{1(K)} &= \frac{1}{3}(-\mu_u + \mu_s), \\
\gamma_{\Sigma^{*+}}^{1(K)} &= \frac{1}{18}(29\mu_u + 16\mu_s), & \gamma_{\Sigma^{*0}}^{1(K)} &= \frac{4}{9}(\mu_u + 2\mu_s), & \gamma_{\Sigma^{*-}}^{1(K)} &= \frac{1}{18}(-13\mu_u + 16\mu_s), \\
\gamma_{\Xi^{*0}}^{1(K)} &= \mu_u + \frac{5\mu_s}{3}, & \gamma_{\Xi^{*-}}^{1(K)} &= \frac{1}{3}(-\mu_u + 5\mu_s), \\
\gamma_{\Omega^-}^{1(K)} &= \frac{1}{6}(\mu_u + 8\mu_s),
\end{aligned} \tag{B6}$$

for the kaon loops, and

$$\begin{aligned}
\gamma_{\Delta^{++}}^{1(\eta)} &= \frac{\mu_u}{2}, & \gamma_{\Delta^+}^{1(\eta)} &= \frac{\mu_u}{4}, & \gamma_{\Delta^0}^{1(\eta)} &= 0, & \gamma_{\Delta^-}^{1(\eta)} &= -\frac{\mu_u}{4}, \\
\gamma_{\Sigma^{*+}}^{1(\eta)} &= 0, & \gamma_{\Sigma^{*0}}^{1(\eta)} &= 0, & \gamma_{\Sigma^{*-}}^{1(\eta)} &= 0, \\
\gamma_{\Xi^{*0}}^{1(\eta)} &= \frac{1}{6}(\mu_u + 2\mu_s), & \gamma_{\Xi^{*-}}^{1(\eta)} &= \frac{1}{12}(-\mu_u + 4\mu_s), \\
\gamma_{\Omega^-}^{1(\eta)} &= 2\mu_s,
\end{aligned} \tag{B7}$$

for the η loops. The coefficients $\tilde{\gamma}_b^1$ evaluated from the graphs 2b are given, up to a factor \mathcal{C}^2 , as follows

$$\begin{aligned}
\tilde{\gamma}_{\Delta^{++}}^{1(\pi)} &= \frac{3}{2}\mu_u, & \tilde{\gamma}_{\Delta^+}^{1(\pi)} &= \frac{2}{3}\mu_u, & \tilde{\gamma}_{\Delta^0}^{1(\pi)} &= -\frac{\mu_u}{6}, & \tilde{\gamma}_{\Delta^-}^{1(\pi)} &= -\mu_u, \\
\tilde{\gamma}_{\Sigma^{*+}}^{1(\pi)} &= \frac{7}{18}(2\mu_u + \mu_s), & \tilde{\gamma}_{\Sigma^{*0}}^{1(\pi)} &= \frac{1}{18}(2\mu_u + 7\mu_s), & \tilde{\gamma}_{\Sigma^{*-}}^{1(\pi)} &= \frac{1}{18}(-10\mu_u + 7\mu_s), \\
\tilde{\gamma}_{\Xi^{*0}}^{1(\pi)} &= \frac{2}{3}\mu_s, & \tilde{\gamma}_{\Xi^{*-}}^{1(\pi)} &= \frac{1}{12}(-\mu_u + 8\mu_s), \\
\tilde{\gamma}_{\Omega^-}^{1(\pi)} &= 0,
\end{aligned} \tag{B8}$$

for the pion loops,

$$\begin{aligned}
\tilde{\gamma}_{\Delta^{++}}^{1(K)} &= \frac{1}{3}(4\mu_u - \mu_s), & \tilde{\gamma}_{\Delta^+}^{1(K)} &= \frac{1}{3}(2\mu_u - \mu_s), & \tilde{\gamma}_{\Delta^0}^{1(K)} &= -\frac{\mu_s}{3}, & \tilde{\gamma}_{\Delta^-}^{1(K)} &= -\frac{1}{3}(2\mu_u + \mu_s), \\
\tilde{\gamma}_{\Sigma^{*+}}^{1(K)} &= \frac{1}{18}(7\mu_u + 8\mu_s), & \tilde{\gamma}_{\Sigma^{*0}}^{1(K)} &= \frac{1}{18}(\mu_u + 8\mu_s), & \tilde{\gamma}_{\Sigma^{*-}}^{1(K)} &= \frac{1}{18}(-5\mu_u + 8\mu_s), \\
\tilde{\gamma}_{\Xi^{*0}}^{1(K)} &= \mu_u + \frac{\mu_s}{3}, & \tilde{\gamma}_{\Xi^{*-}}^{1(K)} &= \frac{1}{3}(-2\mu_u + \mu_s), \\
\tilde{\gamma}_{\Omega^-}^{1(K)} &= \frac{1}{6}(-\mu_u + 16\mu_s),
\end{aligned} \tag{B9}$$

for the kaon loops, and

$$\begin{aligned}
\tilde{\gamma}_{\Delta^{++}}^{1(\eta)} &= 0, & \tilde{\gamma}_{\Delta^+}^{1(\eta)} &= 0, & \tilde{\gamma}_{\Delta^0}^{1(\eta)} &= 0, & \tilde{\gamma}_{\Delta^-}^{1(\eta)} &= 0, \\
\tilde{\gamma}_{\Sigma^{*+}}^{1(\eta)} &= \frac{1}{6}(4\mu_u - \mu_s), & \tilde{\gamma}_{\Sigma^{*0}}^{1(\eta)} &= \frac{1}{6}(\mu_u - \mu_s), & \tilde{\gamma}_{\Sigma^{*-}}^{1(\eta)} &= -\frac{1}{6}(2\mu_u + \mu_s), \\
\tilde{\gamma}_{\Xi^{*0}}^{1(\eta)} &= \frac{1}{6}(-\mu_u + 4\mu_s), & \tilde{\gamma}_{\Xi^{*-}}^{1(\eta)} &= \frac{1}{12}(\mu_u + 8\mu_s), \\
\tilde{\gamma}_{\Omega^-}^{1(\eta)} &= 0,
\end{aligned} \tag{B10}$$

for the η loops. The coefficients $\tilde{\gamma}_b^2$ evaluated from the graphs 2c (or 2d) are given, up to a factor $2\mathcal{CH}/3$, by

$$\begin{aligned}
\tilde{\gamma}_{\Delta^{++}}^{2(\pi)} &= 2\mu_u, & \tilde{\gamma}_{\Delta^+}^{2(\pi)} &= \frac{2}{3}\mu_u, & \tilde{\gamma}_{\Delta^0}^{2(\pi)} &= -\frac{2}{3}\mu_u, & \tilde{\gamma}_{\Delta^-}^{2(\pi)} &= -2\mu_u, \\
\tilde{\gamma}_{\Sigma^{*+}}^{2(\pi)} &= \frac{4}{9}(\mu_u + 2\mu_s), & \tilde{\gamma}_{\Sigma^{*0}}^{2(\pi)} &= \frac{2}{9}(-\mu_u + 4\mu_s), & \tilde{\gamma}_{\Sigma^{*-}}^{2(\pi)} &= \frac{8}{9}(-\mu_u + \mu_s), \\
\tilde{\gamma}_{\Xi^{*0}}^{2(\pi)} &= \frac{2}{3}\mu_s, & \tilde{\gamma}_{\Xi^{*-}}^{2(\pi)} &= \frac{1}{3}(-\mu_u + 2\mu_s), \\
\tilde{\gamma}_{\Omega^-}^{2(\pi)} &= 0,
\end{aligned} \tag{B11}$$

for the pion loops,

$$\begin{aligned}
\tilde{\gamma}_{\Delta^{++}}^{2(K)} &= \frac{4}{3}(\mu_u - \mu_s), & \tilde{\gamma}_{\Delta^+}^{2(K)} &= \frac{2}{3}(\mu_u - 2\mu_s), & \tilde{\gamma}_{\Delta^0}^{2(K)} &= -\frac{4}{3}\mu_s, & \tilde{\gamma}_{\Delta^-}^{2(K)} &= -\frac{2}{3}(\mu_u + 2\mu_s), \\
\tilde{\gamma}_{\Sigma^{*+}}^{2(K)} &= \frac{2}{9}(7\mu_u - 4\mu_s), & \tilde{\gamma}_{\Sigma^{*0}}^{2(K)} &= \frac{2}{9}(\mu_u - 4\mu_s), & \tilde{\gamma}_{\Sigma^{*-}}^{2(K)} &= -\frac{2}{9}(5\mu_u + 4\mu_s), \\
\tilde{\gamma}_{\Xi^{*0}}^{2(K)} &= \frac{4}{3}\mu_s, & \tilde{\gamma}_{\Xi^{*-}}^{2(K)} &= \frac{2}{3}(-\mu_u + 2\mu_s), \\
\tilde{\gamma}_{\Omega^-}^{2(K)} &= \frac{2}{3}(-\mu_u + 4\mu_s),
\end{aligned} \tag{B12}$$

for the kaon loops, and

$$\begin{aligned}
\tilde{\gamma}_{\Delta^{++}}^{2(\eta)} &= 0, & \tilde{\gamma}_{\Delta^+}^{2(\eta)} &= 0, & \tilde{\gamma}_{\Delta^0}^{2(\eta)} &= 0, & \tilde{\gamma}_{\Delta^-}^{2(\eta)} &= 0, \\
\tilde{\gamma}_{\Sigma^{*+}}^{2(\eta)} &= 0, & \tilde{\gamma}_{\Sigma^{*0}}^{2(\eta)} &= 0, & \tilde{\gamma}_{\Sigma^{*-}}^{2(\eta)} &= 0, \\
\tilde{\gamma}_{\Xi^{*0}}^{2(\eta)} &= \frac{2}{3}(\mu_u - \mu_s), & \tilde{\gamma}_{\Xi^{*-}}^{2(\eta)} &= -\frac{1}{3}(\mu_u + 2\mu_s), \\
\tilde{\gamma}_{\Omega^-}^{2(\eta)} &= 0,
\end{aligned} \tag{B13}$$

for the η loops. The group coefficients λ_b evaluated from the graphs 2e, up to a factor \mathcal{H}^2 , are

$$\lambda_{\Delta}^{(\pi)} = \frac{25}{36}, \lambda_{\Sigma^*}^{(\pi)} = \frac{10}{27}, \lambda_{\Xi^*}^{(\pi)} = \frac{5}{36}, \lambda_{\Omega^-}^{(\pi)} = 0, \tag{B14}$$

for the pion loops

$$\lambda_{\Delta}^{(K)} = \frac{5}{18}, \lambda_{\Sigma^*}^{(K)} = \frac{20}{27}, \lambda_{\Xi^*}^{(K)} = \frac{5}{6}, \lambda_{\Omega^-}^{(K)} = \frac{5}{9}, \tag{B15}$$

for the kaon loops, and

$$\lambda_{\Delta}^{(\eta)} = \frac{5}{36}, \lambda_{\Sigma^*}^{(\eta)} = 0, \lambda_{\Xi^*}^{(\eta)} = \frac{5}{36}, \lambda_{\Omega^-}^{(\eta)} = \frac{5}{9}, \quad (\text{B16})$$

for the η loops. The group coefficients $\tilde{\lambda}_b$ evaluated from the graphs 2f, up to a factor \mathcal{C}^2 , are

$$\tilde{\lambda}_{\Delta}^{(\pi)} = \frac{1}{2}, \tilde{\lambda}_{\Sigma^*}^{(\pi)} = \frac{5}{12}, \tilde{\lambda}_{\Xi^*}^{(\pi)} = \frac{1}{4}, \tilde{\lambda}_{\Omega^-}^{(\pi)} = 0, \quad (\text{B17})$$

for the pion loops

$$\tilde{\lambda}_{\Delta}^{(K)} = \frac{1}{2}, \tilde{\lambda}_{\Sigma^*}^{(K)} = \frac{1}{3}, \tilde{\lambda}_{\Xi^*}^{(K)} = \frac{1}{2}, \tilde{\lambda}_{\Omega^-}^{(K)} = 1, \quad (\text{B18})$$

for the kaon loops, and

$$\tilde{\lambda}_{\Delta}^{(\eta)} = 0, \tilde{\lambda}_{\Sigma^*}^{(\eta)} = 1, \tilde{\lambda}_{\Xi^*}^{(\eta)} = \frac{1}{4}, \tilde{\lambda}_{\Omega^-}^{(\eta)} = 0, \quad (\text{B19})$$

for the η loops.

APPENDIX C: THE EXPRESSIONS OF \tilde{F} , L_0 , L_1 , AND L_2

The expressions of $L_0(m, \lambda)$, $\tilde{F}(m, \delta, \lambda)$, $L_1(m_X, \delta, \lambda)$, and $L_2(m_X, \delta, \lambda)$ are given in [2]. In order to get $\tilde{F}(m_X, -\delta, \lambda)$, $L_1(m_X, -\delta, \lambda)$, and $L_2(m_X, -\delta, \lambda)$ from them, we make an analytic continuation from positive to negative δ . Note that the functions can acquire an imaginary part in the continuation, but it will not contribute to the decuplet moments and therefore can be ignored. The real parts of the new functions are obtained by a simple substitution of $-\delta$ for δ .

As an illustration, The function $\tilde{F}(m, -\delta, \lambda)$ is found of the form

$$\begin{aligned} \pi\tilde{F}(m, -\delta, \lambda) = & \frac{\lambda^4}{3(\lambda^2 - m^2 + \delta^2)^2} \left\{ -N(m, -\delta, \lambda) + \frac{5\lambda^2 + 2m^2}{\lambda^2 - m^2}\delta + \frac{\lambda^2 + 2m^2}{(\lambda^2 - m^2)^2}\delta^3 \right. \\ & + \frac{\lambda\delta}{(\lambda^2 - m^2)^2(\lambda^2 - m^2 + \delta^2)} \left[3(2\lambda^2 + 3m^2)(\lambda^2 - m^2) - 2(\lambda^2 - 6m^2)\delta^2 \right. \\ & \left. \left. + \frac{3m^2}{\lambda^2 - m^2}\delta^4 \right] F_0(m, \lambda) \right\} , \end{aligned} \quad (C1)$$

where

$$N(m, -\delta, \lambda) = \frac{1}{(\lambda^2 - m^2 + \delta^2)} \left[\pi\lambda(\lambda^2 + 3m^2 - 3\delta^2) - 2(3\lambda^2 + m^2 - \delta^2) F_0(m, -\delta) \right] , \quad (C2)$$

and

$$F_0(m, \pm\delta) = \sqrt{m^2 - \delta^2} (\pi/2 \mp \arctan [\delta/\sqrt{m^2 - \delta^2}]) \quad \text{for } m \geq \delta , \quad (C3)$$

$$= \sqrt{\delta^2 - m^2} \{ \ln [(\mp\delta + \sqrt{\delta^2 - m^2})/m] - (1 \mp 1)i\pi/2 \} \quad \text{for } m < \delta . \quad (C4)$$

Similarly, the functions $L_1(m, -\delta, \lambda)$, and $L_2(m, -\delta, \lambda)$ can be easily read off from $L_1(m, \delta, \lambda)$, and $L_2(m, \delta, \lambda)$.

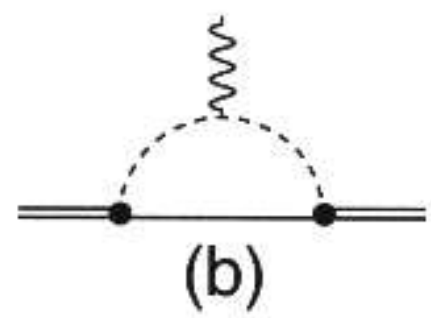
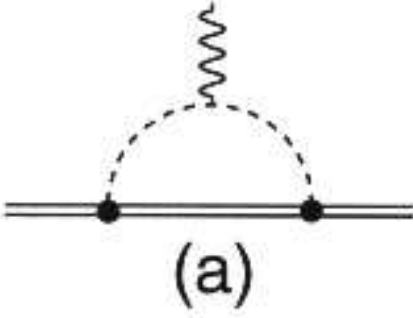
REFERENCES

- [1] L. Durand and P. Ha, Proceedings of the Como Conference on Quark Confinement and Hadron Spectrum II, Eds. N. Brambilla and G.M. Prosperi (World Scientific, Singapore, 1996); hep-ph/9609495.
- [2] L. Durand and P. Ha, submitted to Phys. Rev. **D**.
- [3] E. Jenkins, M. Luke, A.V. Manohar, and M.J. Savage, Phys. Lett. **B302** (1993) 482; (E) *ibid.* **B388** (1996) 866.
- [4] J. Dai, R. Dashen, E. Jenkins, and A.V. Manohar, Phys. Rev. **D53** (1996) 273.
- [5] Ulf-G. Meißner, S. Steininger, Nucl. Phys. **B499** (1997) 349.
- [6] J.W. Bos, D. Chang, S.C. Lee, Y.C. Lin, and H. H. Chin, J. Phys. (Taipei) **35** (1997) 150.
- [7] L. Durand and P. Ha, Phys. Rev. **D** (1998), in press.
- [8] H. Georgi, Phys. Lett. **240B** (1990) 447;
E. Jenkins and A.V. Manohar, Phys. Lett **B255** (1991) 558; UCSD/PTH 91-30.
- [9] M.N. Butler, M.J. Savage, and R.P. Springer, Phys. Rev **D49** (1994) 3459;
Nucl. Phys. **B399** (1993) 69.

FIGURES

FIG. 1. Diagrams that give rise to non-analytic $m_s^{1/2}$ corrections to the baryon magnetic moments in the conventional ChPT. The dashed lines denote the mesons, the single and double solid lines denote octet and decuplet baryons, respectively. A heavy dot with a meson line represents a form factor $F(k, v)$ (Eq.(2.14)), where k is the meson momentum.

FIG. 2. Diagrams that give rise to non-analytic $m_s \ln m_s$ corrections to the baryon magnetic moments in the conventional ChPT.





(a)



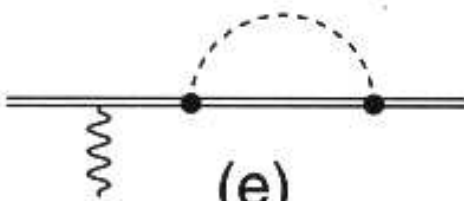
(b)



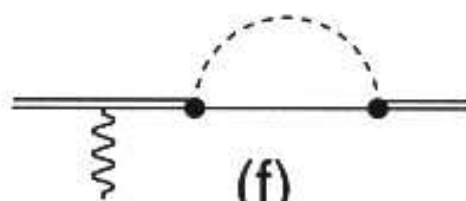
(c)



(d)



(e)



(f)

TABLES

TABLE I. The decuplet magnetic moments from the QM and the QCD-based QM with loop corrections.

μ_b	QM	QM w/ loops	Experiment
Δ^{++}	5.455	5.689	3.5 – 7.5
Δ^+	2.728	2.778	–
Δ^0	0	–0.134	–
Δ^-	–2.728	–3.045	–
Σ^{*+}	3.057	2.933	–
Σ^{*0}	0.329	0.137	–
Σ^{*-}	–2.399	–2.659	–
Ξ^{*0}	0.658	0.424	–
Ξ^{*-}	–2.069	–2.307	–
Ω^-	–1.740	–1.970	–2.02 \pm 0.05

TABLE II. Detailed breakdown of the contributions of the loop integrals to the magnetic moments of the decuplet baryons (in μ_N). Those contributions are evaluated at $F = 0.5$, $D = 0.75$, $\mathcal{C} = -1.5$, $\mathcal{H} = -2.25$, $\delta = 250$ MeV, $\mu_u = 2.083$, $\mu_s = -0.656$ and the natural cutoff $\mu = 407$ MeV.

μ_b	μ_u, μ_s	$\Delta\mu_b^{QM}$	$m_s^{1/2(N)}$	$\ln m_s^{(N)}$	$m_s^{1/2(\Delta)}$	$\ln m_s^{(\Delta)}$	Loops	μ_b
Δ^{++}	6.249	–0.434	0.078	–0.351	0.159	–0.012	–0.126	5.689
Δ^+	3.125	–0.217	0.052	–0.183	0.060	–0.059	–0.130	2.778
Δ^0	0	0	0.026	–0.015	–0.039	–0.106	–0.134	–0.134
Δ^-	–3.125	0.217	0	0.153	–0.138	–0.152	–0.138	–3.045
Σ^{*+}	3.510	–0.343	0.026	–0.192	0.099	–0.167	–0.234	2.933
Σ^{*0}	0.386	–0.089	0	–0.032	0	–0.127	–0.159	0.137
Σ^{*-}	–2.739	0.165	–0.026	0.127	–0.099	–0.087	–0.085	–2.659
Ξ^{*0}	0.771	–0.191	–0.026	–0.052	0.039	–0.117	–0.156	0.424
Ξ^{*-}	–2.354	0.096	–0.052	0.102	–0.060	–0.041	–0.050	–2.307
Ω^-	–1.968	0.013	–0.077	0.077	–0.021	0.006	–0.015	–1.970